

Article ID: 1006-8775(2011) 02-0093-10

## A NUMERICAL DIAGNOSIS OF LEADING SIGNALS FACILITATING A “NORTH-RIDGE SOUTH-TROUGH” DIPOLE FOR THE EARLY-2008 SOUTH-CHINA FREEZING-RAIN EVENTS

WU Jun-jie (吴俊杰)<sup>1,3</sup>, LIN Liang-xun (林良勋)<sup>2</sup>, QIAN Yu-kun (钱钰坤)<sup>1</sup>, YUAN Zhuo-jian (袁卓建)<sup>1</sup>,  
QI Jin-dian (戚锦典)<sup>1</sup>

(1. Center for Monsoon and Environment Research/Department of Atmospheric Science, Sun Yat-sen University, Guangzhou 510275 China; 2. Guangzhou Meteorological Observatory, Guangzhou 510080 China; 3. Civil Aviation Flight University of China, Guanghan, Sichuan 618307 China)

**Abstract:** Previous studies emphasize the important role of a “north-ridge versus south-trough” dipole (affecting the latitudes from 20° to 75° N around the Tibetan Plateau) of anomalous geopotential height ( $Z$ ) in the early-2008 abnormal cryogenic freezing-rain-and-snow events in the southern part of China. The present study intends to extract the leading signal facilitating the dipole based on the numerical outputs of a full  $Z$ -linear model for diagnosing the global  $Z$ . Using this model built on full primitive equations in spherical-isobaric coordinates, we can further split the anomaly of  $Z - Z_{f\zeta-u\beta}$  (representing the  $Z$  component not explicitly associated with the Coriolis parameter  $f$  and its meridional derivative  $\beta$ ) into 15 components. With the model-output  $Z_{f\zeta-u\beta}$  (mainly accounting for the dipole under the geostrophic balance) and  $Z - Z_{f\zeta-u\beta}$  matrices as the left and right singular vectors respectively, a maximum covariance analysis (MCA) is performed to extract the significant 2-4-day leading signal carried by the MCA  $Z - Z_{f\zeta-u\beta}$  mode in the upstream area of the dipole. This leading signal is mainly attributed to 1) the abnormally strong westerlies centered around the exit region of the Atlantic jet-stream and 2) the corresponding anomalous 950-300 hPa anticyclone to the south of the abnormally strong center of westerlies. The energy of the positive wave center around this jet exit region favors the downstream north-ridge while the energy of the negative wave center associated with the anomalous anticyclone favors the downstream south-trough.

**Key words:** blocking system; freezing rain; numerical diagnosis; leading signals

**CLC number:** P435

**Document code:** A

**doi:** 10.3969/j.issn.1006-8775.2011.02.001

### 1 INTRODUCTION

In early 2008 (from 10 January to 2 February), the southern part of China suffered from four abnormal cryogenic freezing-rain-and-snow events<sup>[1]</sup> with the strongest event occurring after 25 January 2008<sup>[2]</sup>. According to previous studies<sup>[2-7]</sup>, these abnormal events are associated with the combined effect of abnormally cold air from the higher latitudes and the abnormally moist air from the lower latitudes. The predominant system behind the phenomena pointed out by most of the studies is the dipole in the anomalous geopotential height ( $Z$ ) field

characterized by a north-ridge and a south-trough extending from 700 hPa to 300 hPa. This dipole (located around the Tibetan Plateau affecting the latitudes from 20° N to 75° N) favors the interaction of active cold air (from the eastern flank of the north-ridge) and the active moist air (ahead of the south-trough) in the southern part of China.

Focusing on the interaction between the general circulation and waves, some studies<sup>[8-10]</sup> have emphasized the positive contribution to the north-ridge by the Rossby wave energy in the upstream area around the northeastern Atlantic and the West Europe. Other study<sup>[11]</sup> has emphasized the

Received 2010-05-13; Revised 2011-02-23; Accepted 2011-04-15

**Foundation item:** National Key Basic Research Project of China (2009CB421404); a key project of Chinese National Science Foundation (40930950; 40730951); Chinese National Science Foundation (40575021); General Program of CAFUC (J2010-29)

**Biography:** WU Jun-jie, Ph.D., primarily undertaking research on numerical diagnosis of atmospheric circulation.

**Corresponding author:** YUAN Zhuo-jian, e-mail: wjj137404@yahoo.com.cn

contribution to the north-ridge by the upstream negative vorticity advection. Paying close attention to the sustained feature of the event, Wu et al.<sup>[7]</sup> have revealed that the early-2008 cryogenic freezing-rain-and-snow events in the southern part of China are positively related to the Madden-Julian Oscillation (MJO) phase characterized by active convection in the equatorial region over the middle Indian Ocean and suppressed convection over Indonesia.

In view of the importance of the “north-ridge versus south-trough” dipole, the present quantitative numerical study tries to extract leading signals for the dipole. Since the dipole is significant in the anomalous  $Z$  field, the linear model for diagnosing global  $Z$  derived by Yuan et al.<sup>[12]</sup> is used to further split the anomaly of  $Z - Z_{f\zeta-u\beta}$  (representing the  $Z$  component not explicitly associated with the Coriolis parameter  $f$  and its meridional derivative  $\beta$ ) into 15 components. Such partitioning is not only based on the linearity of the  $Z$  equation but also based on the perspective that  $Z_{f\zeta-u\beta}$  mostly accounts for the geostrophic balance while  $Z - Z_{f\zeta-u\beta}$  is responsible for changing the balance. So the  $Z - Z_{f\zeta-u\beta}$  might carry the leading signal.

To extract the leading signal carried by  $Z - Z_{f\zeta-u\beta}$ , we first numerically solve the  $Z$  linear model (briefly described in section 2) with reanalysis data (also see section 2). Then we carry out the model validation together with a brief review of the anomalous pattern of  $Z$  characterized by the

$$\begin{aligned} \cos\varphi \sum_{i=1}^{17} f_i = \cos\varphi \left[ \right. & \underbrace{-\frac{\partial}{\partial t} \left\{ \frac{\dot{Q}}{C_p T} - \frac{1}{\theta} \left( \frac{\partial(\omega\theta)}{\partial p} + \frac{\partial\theta}{\partial t} + \mathbf{V}_2 \cdot \nabla\theta \right) \right\}}_1 - \underbrace{\frac{\partial}{\partial x} \left( u \frac{\partial u}{\partial x} \right)}_2 - \underbrace{\frac{1}{\cos\varphi} \frac{\partial}{\partial y} \left( u \cos\varphi \frac{\partial v}{\partial x} \right)}_3 \\ & \underbrace{- \frac{\partial}{\partial x} \left( v \frac{\partial u}{\partial y} \right)}_4 - \underbrace{\frac{1}{\cos\varphi} \frac{\partial}{\partial y} \left( v \cos\varphi \frac{\partial v}{\partial y} \right)}_5 - \underbrace{\omega \frac{\partial}{\partial p} \left\{ \frac{\dot{Q}}{C_p T} - \frac{1}{\theta} \left( \frac{\partial(\omega\theta)}{\partial p} + \frac{\partial\theta}{\partial t} + \mathbf{V}_2 \cdot \nabla\theta \right) \right\}}_6 \\ & \underbrace{- \frac{\partial\omega}{\partial x} \frac{\partial u}{\partial p}}_7 - \underbrace{\frac{\partial\omega}{\partial y} \frac{\partial v}{\partial p}}_8 + \underbrace{f\zeta}_9 - \underbrace{u \frac{df}{dy}}_{10} - \underbrace{\frac{\partial}{\partial x} \left( \frac{u^2 \tan\varphi \cos\varphi}{a} \right)}_{11} + \underbrace{\nabla_2 \cdot \mathbf{F}}_{12} \\ & \left. + \underbrace{\frac{\partial}{\partial x} \left( \frac{uv \tan\varphi}{a} \right)}_{13} + \underbrace{\frac{RT\omega}{pga} \nabla_2 \cdot \mathbf{V}}_{14} + \underbrace{\frac{R}{pga} \left( u \frac{\partial\omega T}{\partial x} + v \frac{\partial\omega T}{\partial y} + \frac{Rf}{pg} \frac{\partial\omega T}{\partial x} \right)}_{15, 16, 17} \right] \end{aligned}$$

The symbols in Eq. (1) are defined as  $f = 2\Omega \sin\varphi$ ,  $\partial x = a \cos\varphi \partial\lambda$ ,  $\partial y = a \partial\varphi$ ,  $a = 6.37 \times 10^6$  m,  $\lambda$  the longitude,  $\varphi$  the latitude,  $\theta$  the potential temperature,  $\zeta$  the relative vorticity,  $\mathbf{F}$  the frictional force and  $\dot{Q}/C_p$  the diabatic heating rate. The left hand side of Eq. (1) is the horizontal divergence of pressure gradient (i.e.,

“north-ridge versus south-trough” dipole (section 3). After using the model to split the observed  $Z$  anomaly into  $Z_{f\zeta-u\beta}$  and the 15 components of  $Z - Z_{f\zeta-u\beta}$ , we apply these model outputs to the maximum covariance analysis (MCA)<sup>[13]</sup> to extract the leading signal carried by the MCA  $Z - Z_{f\zeta-u\beta}$  mode (section 4). Corresponding anomalous systems behind the leading signal are presented in section 5. A summary is given in section 6.

## 2 METHODS AND DATA

The present numerical diagnosis is based on the full  $Z$  linear model derived by Yuan et al.<sup>[12]</sup> for diagnosing the global  $Z$  field. This full  $Z$  equation (built on the full primitive equations in spherical-isobaric coordinates) is an elliptic-type partial differential equation unconditionally since the coefficients of  $Z$ 's second-order derivatives are always positive (i.e.,  $\cos\varphi$ ) in the latitudes away from the poles as shown by Eq. (1).

$$9.8 \cos\varphi \nabla_2^2 Z = \cos\varphi \sum_{i=1}^{17} f_i, \quad (1)$$

where

$$\cos\varphi \nabla_2^2 Z = \frac{\partial}{\partial x} \left( \cos\varphi \frac{\partial Z}{\partial x} \right) + \frac{\partial}{\partial y} \left( \cos\varphi \frac{\partial Z}{\partial y} \right)$$

and

$9.8 \nabla_2 \cdot \nabla_2 Z = 9.8 \nabla_2^2 Z$ ) multiplied by  $\cos\varphi$ . The purpose of multiplying  $9.8 \nabla_2^2 Z$  by  $\cos\varphi$  is to generate a flux form of  $Z$ 's numerical model and to reduce the errors caused by solving the non-flux form of  $Z$ 's model of

$$\nabla^2 Z = \frac{\partial^2 Z}{\partial x^2} + \frac{1}{\cos \varphi} \frac{\partial}{\partial y} \left( \cos \varphi \frac{\partial Z}{\partial y} \right) = \frac{1}{9.8} \sum_{i=1}^{17} f_i$$

with finite difference schemes and gridded data.

### 2.1 Data and domains used in the present study

The data used in the present numerical diagnosis and statistical and synoptic analyses are the reanalysis data with  $2.5^\circ \times 2.5^\circ$  latitude-longitude resolution provided by the National Center for Environmental Prediction/National Center for Atmospheric Research (NCEP/NCAR, USA)<sup>[14, 15]</sup>. Based on the NCEP/NCAR gridded data and the linearity of Eq. (1) in terms of  $Z$ , the anomaly of  $Z_{obs}$  (representing the observed  $Z$ ) defined by  $Z'_{obs} = Z_{obs} - \overline{Z_{obs}}$  can be partitioned into:

$$Z'_{obs} = (Z_b - \overline{Z_b}) + \sum_{i=1}^{17} (Z_i - \overline{Z_i}) = Z'_b + \sum_{i=1}^{17} Z'_i$$

where  $\overline{Z_{obs}}$  stands for the long-term mean and  $Z_b$  is attributed to the boundary effect (providing little insight, though)<sup>[12]</sup>. Each  $Z'_i$  ( $i=1, 2, \dots, 17$ ), attributed to the  $i$ th right-hand-side (rhs) term  $f'_i$  can be calculated by solving  $9.8\nabla^2 Z'_i = f'_i$  with  $Z'_i = 0$  at the boundaries of the numerical model domain (i.e., the whole Northern Hemisphere (NH)). For the sake of convenience, we drop the superscript “'” thereafter. The quantitative comparison of model-output  $Z_i$  ( $i=1, 2, \dots, 17$ ) is then carried out to determine the major contributor of  $Z_{obs}$  at different stages of weather and climate changes in the whole NH. Hence, the northern and southern boundaries of the model domain are respectively located at the Equator and the North Pole. The zonal boundary is periodic.

However, in the model-output statistical analyses, we only focus on the upstream region ( $40^\circ$  W– $60^\circ$  E,  $20$ – $70^\circ$  N) with significant leading signals carried by  $Z_2 + Z_{3+4}$  and the downstream region ( $50$ – $140^\circ$  E,  $20$ – $70^\circ$  N) with an obvious dipole in the  $Z_{f\zeta-u\beta}$  field. The model-output  $Z_{f\zeta-u\beta}$  and  $Z_2 + Z_{3+4}$  fields are analyzed statistically based on the MCA for extracting the leading signal since  $Z_{f\zeta-u\beta}$  accounts for the main feature of the geostrophic pattern and  $Z_2 + Z_{3+4}$  for the main feature of the ageostrophic pattern. The empirical orthogonal function (EOF) analysis is applied to the investigation of anomalous systems behind the leading signal in the upstream region ( $40^\circ$  W– $40^\circ$  E,  $20$ – $70^\circ$  N) of the dipole and in

the combined upstream and downstream region ( $40^\circ$  W– $140^\circ$  E,  $10$ – $70^\circ$  N).

### 2.2 The Calculation of forcing terms

The forcing terms on the rhs of Eq. (1) are calculated with the central difference scheme and the NCEP/NCAR gridded data. The diabatic heating rate, i.e.  $Q$  in the rhs term of Eq. (1), is only associated with latent heating, sensible heat flux and latent heat flux since there are no radiative data at each pressure level. The latent heating rate is estimated with the formula:

$$Q_{LH} = -L \left[ \frac{\partial q}{\partial t} + \nabla \cdot (q\mathbf{V}) + \frac{\partial(q\omega)}{\partial p} \right] \quad (2)$$

given by Yanai et al.<sup>[16]</sup>, where  $L$  is latent heat of condensation,  $q$  the specific humidity,  $\mathbf{V}$  the horizontal velocity vector and  $\omega$  the vertical velocity.

The sensible heat flux  $H_S$ , latent heat flux  $H_L$ , and the frictional stress  ${}_{\nu}\boldsymbol{\tau}$  are described in the conventional sense:

$$H_S = c_p \rho C_D |V_{10m}| (T_s - T_{2m})$$

$$H_L = L \rho C_D |V_{10m}| (q_s - q_{2m})$$

$${}_{\nu}\boldsymbol{\tau} = \rho C_D |V_{10m}| \mathbf{V}_{10m}$$

where  $\rho$  is the air density,  $C_D = 2 \times 10^{-3}$  the drag coefficient<sup>[17, 18]</sup>,  $|V_{10m}|$  the absolute value of the horizontal wind of 10 m above the surface,  $T_s$  the temperature at sea surface,  $T_{2m}$  the temperature of 2 m above the surface,  $q_s$  the specific humidity at the sea surface and  $q_{2m}$  the specific humidity of 2 m above the surface. The frictional force  $\mathbf{F}$  representing the dynamic effect of planetary boundary layer (PBL) is determined by<sup>[19]</sup>

$$\mathbf{F} = \frac{1}{\rho} \frac{\partial {}_{\nu}\boldsymbol{\tau}}{\partial z} \approx \frac{1}{\rho} \frac{0 - {}_{\nu}\boldsymbol{\tau}}{\Delta z} \quad (3)$$

with the absence of frictional stress  ${}_{\nu}\boldsymbol{\tau}$  at the top of the friction active layer.  $\Delta z$  is the thickness of PBL. Since the present study focuses on the 300-hPa  $Z$ , there is no direct impact from the PBL heat fluxes and frictional force on the 300-hPa  $Z$ .

### 2.3 The numerical method and the synoptic information carried by the forcing terms of interest

The finite difference equation corresponding to Eq. (1) (based on a central difference scheme) can be

solved numerically by the successive over relaxation (SOR) iteration method<sup>[12, 20]</sup>. The advantage of Eq. (1) over the classical divergence equation is that each rhs term carries synoptic information. For example, according to Yuan et al.<sup>[12]</sup>, solving  $9.8\nabla_2^2 Z_2 = -\partial(u\partial u/\partial x)/\partial x = f_2$  (with  $Z_2 = 0$  at the boundaries of the model domain) yields the pattern of  $Z_2$  (the contribution to  $Z$  attributed to term 2) characterized by a “+ - +” wave train with  $Z_2 > 0$  around the entrance and exit regions and  $Z_2 < 0$  around the jet-core region based on the linearity of Eq. (1). These results are reasonable; since going monotonously downhill from the higher  $Z_2$  around the entrance region to the lower  $Z_2$  around the jet-core region might cause the air parcel to accelerate and going monotonously uphill from the lower  $Z_2$  around the jet-core region to the higher  $Z_2$  around the exit region might make the air parcel decelerate.

Solving

$$9.8\nabla_2^2 Z_{3+4} = -\partial(u \cos \varphi \partial v / \partial x) / \partial y \\ - \cos \varphi \partial(v \partial u / \partial y) / \partial x = f_3 + f_4$$

yields a  $Z_{3+4}$  pattern being characterized by  $Z_{3+4} > 0$  at the saddle center and  $Z_{3+4} < 0$  in the surrounding regions that are occupied by two pairs of cyclonic-and-anticyclonic circulations<sup>[12]</sup>. These results are consistent with observations that the development of a cyclonic system has no upper-bound

while that of an anticyclonic system might be suppressed after the anticyclone’s intensity reaches a certain level. These components (i.e.,  $Z_2$  and  $Z_{3+4}$ ) are reviewed here since they are the dominant ageostrophic components among the 15 components of  $Z - Z_{f\zeta - u\beta}$  in the freezing-rain events of interest. It is worth mentioning that there is no obvious cancellation between  $Z_2$  and  $Z_{3+4}$ .

### 3 A BRIEF SYNOPTIC REVIEW AND MODEL VALIDATION

A number of studies point out that during the early 2008 abnormal cryogenic freezing-rain-and-snow events in the southern part of China, the abnormally cold air from the eastern flank of the north-ridge of the dipole favors the formation of the abnormally cold surface layer. The abnormally moist air ahead of the south-trough of the dipole favors the abnormal rain and snow. Rain drops fall down into the abnormally cold surface layer to form freezing rain and ice. The important role of the “north-ridge versus south-trough” dipole in the events of interest can be demonstrated by comparing the anomalous  $Z$  patterns in two opposite cases (Fig. 1). Fig. 1b shows that in the 1987 case, an opposite weather situation characterized by relatively warm and dry winter<sup>[21, 22]</sup>, the anomalous 300-hPa  $Z$  pattern (the departure from the mean over the same period as that in the 2008 case, i.e., for 10 January to 2 February) is completely opposite to that in the 2008 case (Fig. 1a) in the region to the west of 120° E.

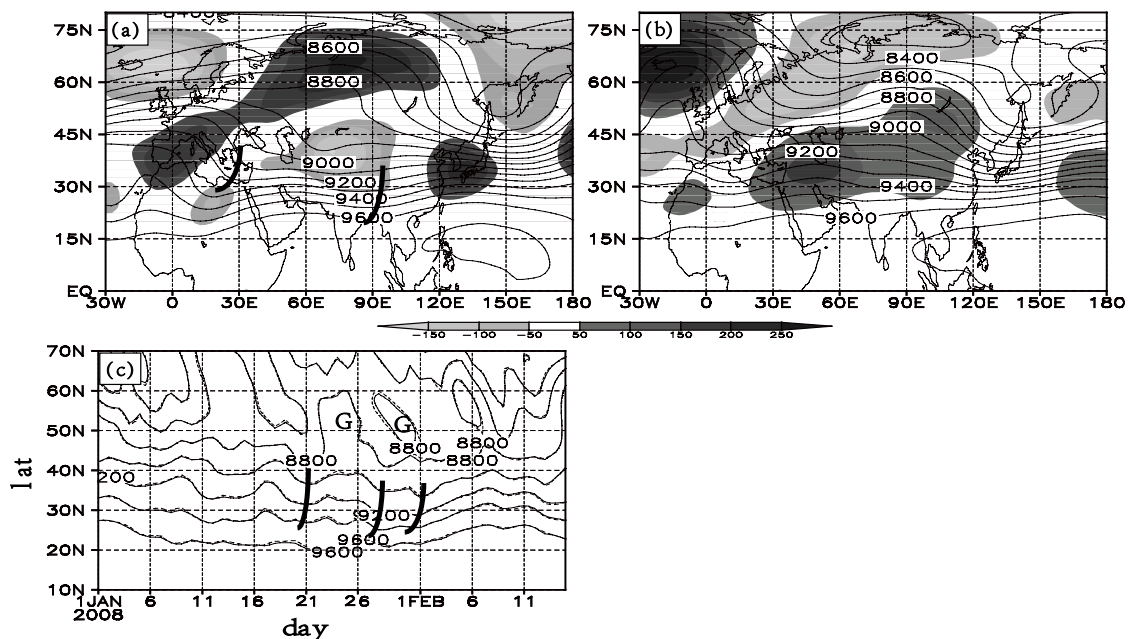


Fig. 1. The (10 January–2 February) time-mean 300-hPa  $Z$  (gpm, solid line) and the corresponding anomalies (gpm, with darker areas for positive anomalies) for (a) 2008 and (b) 1987. (c) The time-meridional section of the observed (solid) and simulated (dashed) 300-hPa  $Z$  along 100° E. The thick lines in (a) and (c) represent the locations of troughs.

In early 2008, the variation of the observed 300-hPa  $Z$  along  $100^\circ$  E in the time-meridional section (Fig. 1c, solid) clearly shows the north-ridge and south-trough pattern in the late January and early February. These observed features (Fig. 1c, solid) have been reasonably simulated (Fig. 1c, dashed) by the full  $Z$  model, i.e. Eq. (1). The simulated  $Z$  field is obtained by solving Eq. (1) with all the internal forces  $f_i$  ( $i=1, 2, \dots, 17$ ) and non-zero boundary values of  $Z$  at the Equator and the North Pole (given by the NCEP/NCAR). Be aware that the zonal boundary is periodic since the model domain is the whole NH. Fig. 1c is plotted with the results of 91 simulations carried out respectively for the observed daily  $Z$  fields in the NH from 1 December 2007 to 29 February 2008. In view of Fig. 1c, we might consider that the following results of numerical diagnosis are trustworthy based on the numerical outputs of Eq. (1).

#### 4 RESULTS OF MODEL-OUTPUT STATISTICAL ANALYSIS

To our knowledge, weather and climate changes result from the variation of geostrophic balance (mainly represented by  $Z_{f\zeta-u\beta}$ ) due to the non-zero effect of ageostrophic processes (mainly represented by  $Z - Z_{f\zeta-u\beta}$ ). Therefore,  $Z - Z_{f\zeta-u\beta}$  might carry leading signals. To extract such leading signals from the observations, we carry out a statistical study based on the MCA with the model-output  $Z_{f\zeta-u\beta}$ -anomaly matrix as the left singular vector and  $Z - Z_{f\zeta-u\beta}$ -anomaly matrix as the right singular vector (Fig. 2).

The MCA results show that only 2-to-4-day leading signal carried by the MCA  $Z - Z_{f\zeta-u\beta}$  mode is significant (indicated by the thickened segment of the open-circle line above the solid line representing the 95% confidence level in Fig. 2a). In the present study, only the upstream MCA  $Z - Z_{f\zeta-u\beta}$  mode (Fig. 2c) carrying 3-day leading signal [referred to as MCA (+3)  $Z - Z_{f\zeta-u\beta}$  mode] is presented together with the downstream MCA  $Z_{f\zeta-u\beta}$  mode (Fig. 2b) [referred to as MCA (+3)  $Z_{f\zeta-u\beta}$  mode]. Consistent with common knowledge, the MCA (+3)  $Z_{f\zeta-u\beta}$  mode (Fig. 2b) is characterized by a “north-ridge versus south-trough” dipole according to the positive expansion coefficient (Fig. 2d, dashed) of the MCA (+3)  $Z_{f\zeta-u\beta}$  mode

during 18 January–6 February 2008. This dipole is similar to the dipole shown in the observed anomalous geopotential height field (Fig. 1a).

The MCA (+3)  $Z - Z_{f\zeta-u\beta}$  mode (Fig. 2c) is characterized by a southwest-to-northeast oriented “+−+” wave train according to the positive expansion coefficient (Fig. 2d, solid) of the MCA (+3)  $Z - Z_{f\zeta-u\beta}$  mode during 17 January–3 February 2008. This wave pattern is similar to the  $Z_2$  wave patterns attributed to jets<sup>[12]</sup>. The correlation between the time series of the MCA(+3)  $Z - Z_{f\zeta-u\beta}$  mode and that of 15 individual components of  $Z - Z_{f\zeta-u\beta}$  reveals that only two correlation coefficients reach the 99% confidence level (Table 1). One correlation is between the  $Z - Z_{f\zeta-u\beta}$  mode and  $Z_{2+5}$ , and the other is between the  $Z - Z_{f\zeta-u\beta}$  mode and  $Z_{3+4}$ . These quantitative comparisons suggest that the abnormally strong westerlies, centered around the exit region of the Atlantic jet stream, and the corresponding anomalous anticyclone, to the south of this abnormally strong center of westerlies, be the systems behind the MCA(+3)  $Z - Z_{f\zeta-u\beta}$  leading signal.

Table 1. Correlation coefficients between the time series of MCA(+3)  $Z - Z_{f\zeta-u\beta}$  mode and that of each major contributor by projecting the contribution of each major contributor onto the MCA(+3)  $Z - Z_{f\zeta-u\beta}$  mode (asterisks denoting the coefficients at 99% confidence level) based on the model-output 300 hPa  $Z$

	$Z$ attributed to each major non- $f\zeta-u\beta$ term					
	$Z_1$	$Z_{2+5}$	$Z_{3+4}$	$Z_6$	$Z_7$	$Z_8$
Correlation coefficient	0.3	0.59*	0.60*	-0.22	-0.33	0.16

#### 5 THE ANOMALOUS SYSTEMS BEHIND THE LEADING SIGNALS

The above results of MCA can be justified by the EOF analysis based on the observational information provided by the NCEP/NCAR in the upstream region ( $40^\circ$  W– $40^\circ$  E,  $20^\circ$ – $70^\circ$  N) of the dipole. The two leading EOF modes of the 300-hPa zonal wind anomaly account for 26.2% and 18.6% of the total variance, respectively (Figs. 3a & 3b). The spatial pattern of the first EOF mode (Fig. 3a) is characterized by a relatively strong center located around the exit region on the anticyclonic shear side of the Atlantic jet stream (the upper-left shaded area

in Fig. 3). This center is an abnormally strong westerly wind center together with the abnormal easterly wind to its south due to the positive expansion coefficient (Fig. 3c dashed) of the first

mode during 1 January–6 February 2008. This pattern suggests that there exists an anomalous anticyclonic circulation centered over the European coastal area.

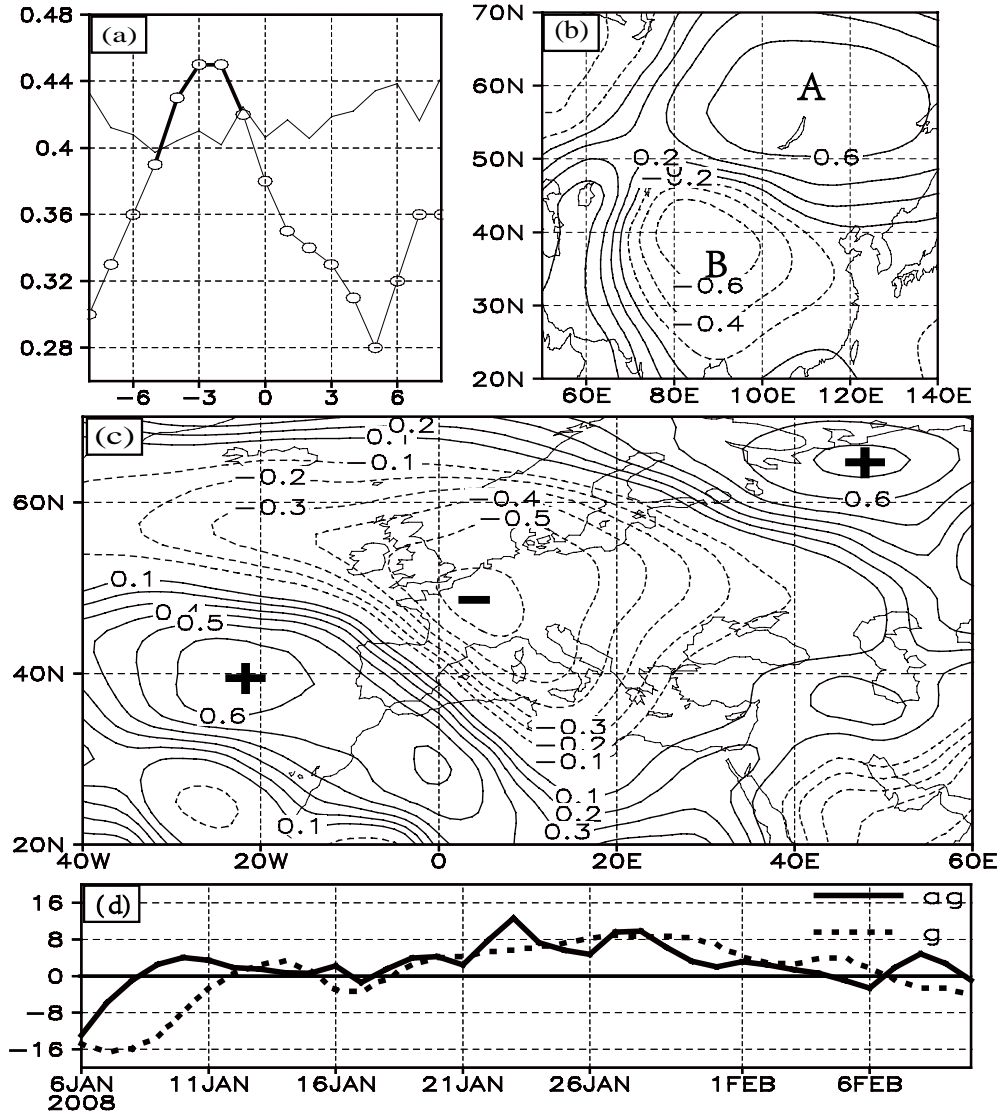


Fig. 2. a: Covariance of the first MCA mode between  $Z_{f\zeta-u\beta}$  and  $Z - Z_{f\zeta-u\beta}$  anomalies. The negative values on the left hand side of the origin indicate that the  $Z - Z_{f\zeta-u\beta}$  mode leads the  $Z_{f\zeta-u\beta}$  mode where the thin solid line in (a) indicates that the covariance is statistically significant at the 5% level; b: Heterogeneous  $Z_{f\zeta-u\beta}$  anomaly; c: Homogeneous  $Z - Z_{f\zeta-u\beta}$  anomaly of the first MCA mode with the  $Z - Z_{f\zeta-u\beta}$  anomaly leading the  $Z_{f\zeta-u\beta}$  anomaly by 3 days, i.e. MCA(+3); d: Time series of the MCA(+3)  $Z_{f\zeta-u\beta}$  mode (dashed line) and the MCA(+3)  $Z - Z_{f\zeta-u\beta}$  mode (solid line). The  $Z_{f\zeta-u\beta}$  and  $Z - Z_{f\zeta-u\beta}$  anomalies are obtained by solving Eq. (1) with the NCEP data from 1 December 2007 to 29 February 2008.

The spatial pattern of the second EOF mode (Fig. 3b) is characterized by a relatively strong center located around ( $60^\circ$  N,  $5^\circ$  W) around the exit region of the Atlantic jet stream. This center is an abnormally strong westerly wind center together with abnormal easterly wind to its south due to the positive expansion coefficient (Fig. 3c solid) of the second mode during 16 January–1 February 2008. This

pattern not only suggests that there exists an anomalous anticyclonic circulation centered in the higher latitude (as compared to the location of the first EOF mode's anticyclone) but also suggests that the latitudes as high as those of the location of the downstream north-ridge be affected by the Atlantic jet stream.

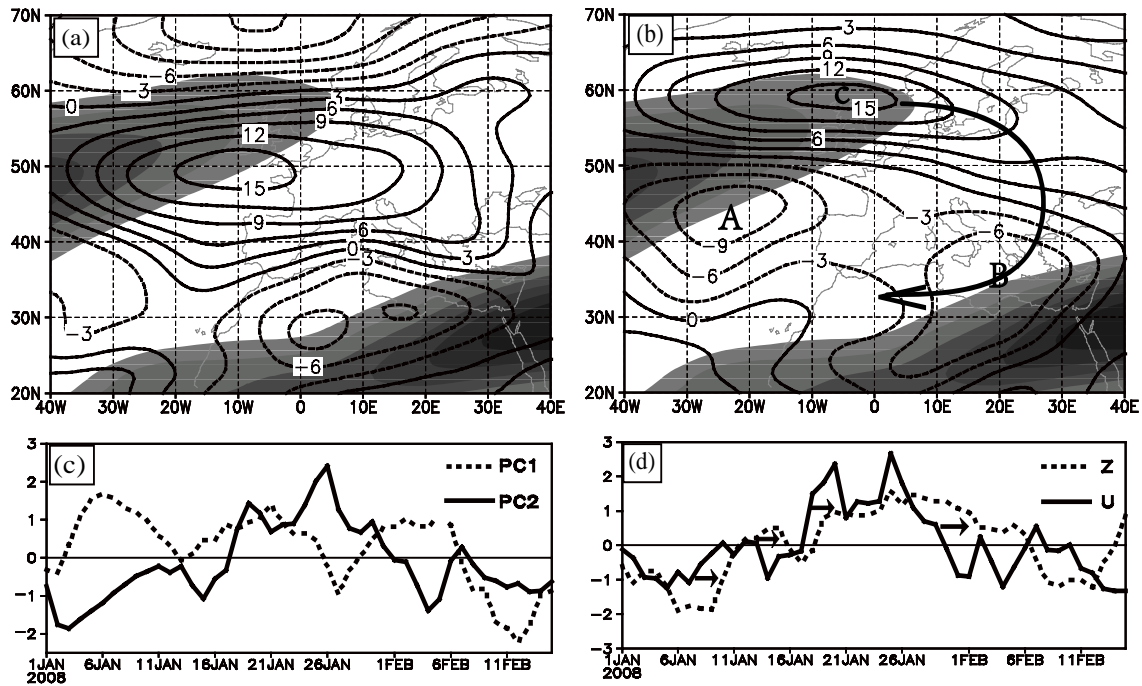


Fig. 3. Two leading EOF modes of 300-hPa zonal wind ( $u$ ) anomaly deviating from the (1 December 2007–29 February 2008) time-mean  $\bar{u}$  (with  $\bar{u} \geq 20 \text{ m s}^{-1}$  shaded). a: The first mode accounts for 26.2% of the total variance; b: The second mode for 18.6%; c: The time series of the first (dashed) and the second (solid) EOF modes; d: Standardized time series of a Z-index (dashed, obtained by subtracting the observed Z at point B from that at point A in Fig. 2b) and a  $u$ -index (solid, obtained by subtracting the observed  $u$  at point B from that at point C in Fig. 3b)

The abnormally strong westerlies centered around the exit region of the Atlantic jet stream might be one of the anomalous systems behind the leading signal carried by the MCA(+3)  $Z - Z_{f\zeta-u\beta}$  mode favorable for the downstream north-ridge. This result can be further justified by the comparison (Fig. 3d) between the variations of the observed  $u$ -index (obtained by subtracting the observed  $u$  at point B from the observed  $u$  at point C in Fig. 3b) and the observed Z-index (obtained by subtracting the observed Z at point B from the observed Z at point A in Fig. 2b) with the  $u$ -index (solid line in Fig. 3d) leading the Z-index (dashed line in Fig. 3d). The corresponding lead-lag correlation coefficient is 0.71 at the 99% confidence level.

The following conclusion might be drawn through summarizing the physical interpretation of  $Z_2$  (see subsection 2.3) together with numerical output, MCA (Fig. 2c), EOF (Fig. 3b) and the above observational analyses (Fig. 3d). The small-scale wave energy of the positive  $Z - Z_{f\zeta-u\beta}$  wave center around the exit region of the Atlantic jet stream facilitates the north-ridge of the large-scale dipole through energy supply. This conclusion can be visualized by Fig. 4 which shows that the small-scale  $Z_2$  disturbance leads the large-scale  $Z_{f\zeta-u\beta}$  dipole. This conclusion

is consistent with those in previous studies<sup>[23, 24]</sup> demonstrating the enhancement of blocking systems after these blocking systems absorb the transient wave energy.

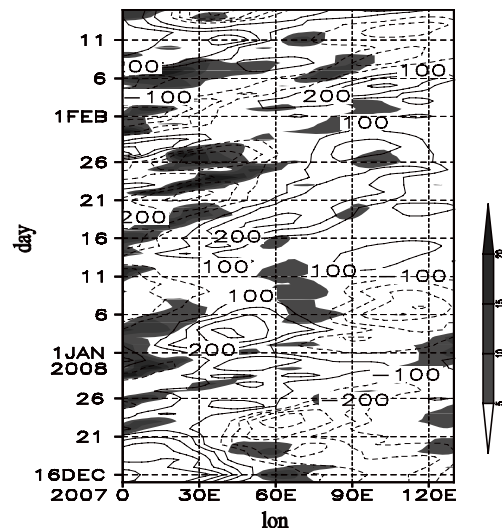


Fig. 4. Time-zonal section of  $Z_2$  anomaly (with anomalous  $Z_2 \geq 5 \text{ gpm}$  shaded) attributed to the jet effect (term 2) and  $Z_{f\zeta-u\beta}$  anomaly (gpm, solid for  $Z_{f\zeta-u\beta} > 0$  and dashed for  $Z_{f\zeta-u\beta} < 0$ ) mostly accounting for the dipole under the geostrophic balance (term 9 and term 10) along  $60^\circ \text{ N}$



Now let us turn our attention to the south-trough of the dipole. Based on the time series of the second EOF mode of  $u$  anomaly in the combined upstream and downstream region ( $40^{\circ}$  W– $140^{\circ}$  E,  $10^{\circ}$ – $70^{\circ}$  N), both regression  $Z$  fields at 300 hPa (Fig. 5a) and 925 hPa (Fig. 5b) recover the anticyclonic system suggested by Fig. 3b. Figs. 5a and 5b indicate that the anomalous anticyclonic system over the European coastal area is a very deep barotropic system. The enhanced mass discharge in this anomalous anticyclonic system, together with the abnormally cold temperature (Fig. 3c, during 11 January–2 February 2008 at point A in Fig. 3b), favors an upper-layer trough. This trough is indicated by the negative (dashed line) centers in Fig. 5d around 21 January and 24 January. After this disturbance's energy is propagated by the 300-hPa westerly wind<sup>[25, 26]</sup> (with a speed of  $35 \text{ m s}^{-1}$  and highlighted by a thick solid line in Fig. 5a), the south-trough (along  $95^{\circ}$  E) significantly intensified after 25 January 2008 (indicated by the shaded area in Fig. 5d). Besides, the enhancement of the south-trough is also positively associated with the MJO activity, which is characterized by the active convection in the equatorial region over the middle Indian Ocean and the suppressed convection over Indonesia<sup>[7]</sup>.

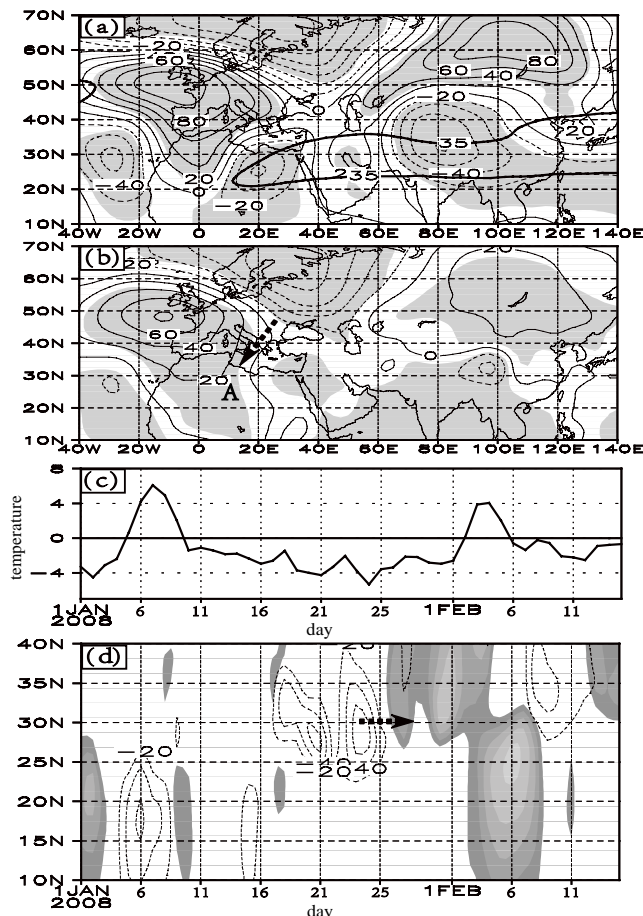


Fig. 5. Regression  $Z$  fields at (a) 300 hPa and (b) 925 hPa based on the time series of the second EOF mode of 300-hPa

$u$  anomaly (with significance exceeding the 95% confidence level shaded) and the (1 December 2007–29 February 2008) time-mean 300-hPa westerly-wind speed of  $35 \text{ m s}^{-1}$  highlighted by the thick solid line). c: Time series of 925-hPa air-temperature anomaly at ( $25^{\circ}$  N,  $15^{\circ}$  E); d: Time-meridional section of strong negative centers of  $Z_{3+4}$  anomalies along  $20^{\circ}$  E (dashed) and along  $95^{\circ}$  E (shaded).

## 6 SUMMARY

A “north-ridge versus south-trough” dipole, located around the Tibetan Plateau affecting the latitudes from  $20^{\circ}$  N to  $75^{\circ}$  N, is clearly identified in the anomalous geopotential-height ( $Z$ ) field by previous studies on the early-2008 abnormal cryogenic freezing-rain-and-snow events in the southern part of China. The dominant role of this dipole, as emphasized by previous studies on the early-2008 abnormal cold-and-wet winter, has been confirmed by a case of relatively warm-and-dry winter of 1987, in which an opposite dipole characterized by a “north-trough versus south-ridge” pattern affected the same region during the same period of interest. Different from previous studies, the present study focuses on the numerical diagnosis of the leading signal facilitating the anomalous  $Z$  dipole in the 2008 case. This numerical diagnosis is based on a full  $Z$  linear diagnostic model derived by Yuan et al.<sup>[12]</sup> with the use of full primitive equations.

This  $Z$  model is able to simulate the observed global  $Z$  field reasonably well. The linearity of this  $Z$  model enables us to split the observed  $Z$  anomaly into  $Z_{f\zeta-u\beta}$  (mainly accounting for the dipole under the geostrophic balance) and 15 components of  $Z - Z_{f\zeta-u\beta}$ . Among these 15 components of  $Z - Z_{f\zeta-u\beta}$ ,  $Z_2$  accounts for the “+ - +” wave trains around jets due to the mass accumulation in the entrance and exit regions of jets<sup>[12]</sup>. This distribution of  $Z_2$  is consistent with observations; as going monotonously downhill from the higher  $Z_2$  around the entrance region to the lower  $Z_2$  in the jet-core region, an air parcel might accelerate and as going monotonously uphill from the lower  $Z_2$  around the jet-core region to the higher  $Z_2$  in the exit region, the air parcel might decelerate.

Among these 15 components of  $Z - Z_{f\zeta-u\beta}$ ,  $Z_{3+4}$  accounts for the higher  $Z_{3+4}$  in the central region of a saddle and lower  $Z_{3+4}$  in the saddle's surrounding regions occupied by two pairs of closed cyclonic and anticyclonic circulations<sup>[12]</sup>. These results can be used to interpret the observations that



further spin-up occurs in cyclonic systems without any upper bound but not in anticyclonic systems.

Since  $Z_{f\zeta-u\beta}$  mainly stands for the geostrophic balance while  $Z - Z_{f\zeta-u\beta}$  is responsible for changing the balance, the above isolation is useful for identifying the ageostrophic processes which might carry leading signals. Based on the NCEP/NCAR gridded data and central difference scheme, the full  $Z$  equation is solved by the SOR iteration method to produce the anomalies of  $Z_{f\zeta-u\beta}$  and 15 components of  $Z - Z_{f\zeta-u\beta}$  in the whole NH. With these model-output 300-hPa  $Z_{f\zeta-u\beta}$  matrix as the left singular vector and  $Z - Z_{f\zeta-u\beta}$  matrix as the right singular vector, the MCA statistical study reveals the significant 2-4-day leading signal carried by the MCA  $Z - Z_{f\zeta-u\beta}$  mode in the upstream region. This leading signal is mainly attributed to the abnormally strong westerlies in the exit region of the Atlantic jet stream and the corresponding anomalous anticyclone to the south of this abnormally strong center of westerlies. The small-scale wave energy of the positive wave center (mainly attributed to  $Z_2$ ) around the exit region of the Atlantic jet stream facilitates the north-ridge of the large-scale dipole through energy supply.

The enhanced mass discharge in the anomalous anticyclonic system (mainly attributed to  $Z_{3+4}$ ) to the south of the abnormally strong center of westerlies, together with the abnormally cold temperature during 11 January–2 February 2008, favors an upper-layer trough located around ( $25^\circ$  N,  $15^\circ$  E). After this disturbance's energy is propagated by the upper-layer westerly wind, the south-trough located around  $95^\circ$  E significantly intensified after 25 January 2008. Besides, the enhancement of the south-trough is also positively associated with the MJO activity characterized by active convection in the equatorial region over the middle Indian Ocean and suppressed convection over Indonesia<sup>[7]</sup>.

## REFERENCES:

[1] WANG Lin, GAO Ge, ZHANG Qiang, et al. Analysis of the severe cold surge, ice-snow and frozen disasters in South China during January 2008: I. climatic features and its impact [J]. Meteor. Mon., 2008, 34(4): 95-100.  
 [2] TAO Shi-yan, WEI Jie. Severe snow and freezing-rain in January 2008 in the southern China [J]. Clim. Env. Res., 2008, 13(4): 337-350.  
 [3] LI Chong-yin, YANG Hui, GU Wei. Cause of severe weather with cold air, freezing rain and snow over south China in January 2008 [J]. Clim. Env. Res., 2008, 13(2): 113-122.  
 [4] GU Lei, WEI Ke, HUANG Rong-hui. Severe disaster of blizzard, freezing rain and low temperature in January 2008 in

China and its associated with the anomalies of East Asian monsoon system [J]. Clim. Env. Res., 2008, 13(4): 405-418.  
 [5] LIN Liang-xun, WU Nai-geng, CAI An-an, et al. Disaster and emergency response of the cryogenic freezing rain and snow weather in Guangdong in 2008 [J]. Meteor. Mon., 2009, 35(5): 26-33.  
 [6] GAO An-ning, CHEN Jian, LI Sheng-yan, et al. Causation analysis of a rare chilling damage in the west of south China in 2008 [J]. J. Trop. Meteor., 2009, 25(1): 110-116.  
 [7] WU Jun-jie, YUAN Zhuo-jian, QIAN Yu-kun, et al. The role of intraseasonal oscillation in the southern-China snowstorms during January 2008 [J]. J. Trop. Meteor., 2009, 25: 103-112.  
 [8] BUEH Cholaw, JI Li-ren, SHI Ning. On the medium-range process of the rainy, snowy and cold weather of south China in early 2008 Part I: Low-frequency waves embedded in the Asian-African subtropical jet [J]. Clim. Env. Res., 2008, 13(4): 419-433.  
 [9] SHI Ning, BUEH Cholaw, JI Li-ren, et al. On the medium-range process of the rainy, snowy and cold weather of south China in early 2008 Part II: Characteristics of the western Pacific subtropical high [J]. Clim. Env. Res., 2008, 13(4): 434-445.  
 [10] JI Li-ren, BUEH Cholaw, SHI Ning, et al. On the medium-range process of the rainy, snowy and cold weather of south China in early 2008 Part III: Pressure trough over the Tibetan Plateau/Bay of Bengal [J]. Clim. Env. Res., 2008, 13(4): 446-458.  
 [11] WANG Dong-hai, LIU Chong-jian, LIU Ying, et al. A preliminary analysis of features and causes of the snow storm event over the Southern China in January 2008 [J]. Acta Meteor. Sinica, 2008, 66(3): 405-422.  
 [12] YUAN Z J, WU J J, CHENG X H, et al. The derivation of a numerical diagnostic model for the forcing of the geopotential [J]. Quart. J. Roy. Meteor. Soc., 2008, 134: 2 067-2 078.  
 [13] CZAJA A, FRANKIGNOUL C. Influence of the North Atlantic SST anomalies on the atmospheric circulation [J]. Geophys. Res. Lett., 1999, 36: 2 969-2 972.  
 [14] KALNAY E, KANAMITSU M, KISTLER R, et al. The NCEP/NCAR 40-year reanalysis project [J]. Bull. Amer. Meteor. Soc., 1996, 77: 437-471.  
 [15] KISTLER R, KALNAY E, COLLINS W, et al. The NCEP-NCAR 50-year reanalysis: monthly means CD-ROM and documentation [J]. Bull. Amer. Meteor. Soc., 2001, 82: 247-267.  
 [16] YANAI M, ESBENSEN S, CHU J-H. Determination of bulk properties of tropical cloud clusters from large-scale heat and moisture budgets [J]. J. Atmos. Sci., 1973, 30: 611-627.  
 [17] DELSOL F, MIYAKODA K, CLARKE R H. Parameterized processes in the surface boundary layer of an atmospheric circulation model [J]. Quart. J. Roy. Meteor. Soc., 1971, 97: 181-208.  
 [18] HOLLOWAY JR. J L, MANABE S. Simulation of climate by a global general circulation model. I. Hydrologic cycle and heat balance [J]. Mon. Wea. Rev., 1971, 99: 335-370.  
 [19] SMAGORINSKY J, MANABE S, HOLLOWAY J L Jr. Numerical results from a nine-level general circulation model of the atmosphere [J]. Mon. Wea. Rev., 1965, 93: 727-768.  
 [20] YUAN Zhuo-jian, WANG Tong-mei, GUO Yu-fu. A numerical simulation of local-zonal-mean Hadley circulation over East Asian I. Schemes [J]. Acta Sci. Nat. Univ. Sunyatseni, 2000, 39(6): 112-116.  
 [21] QIN Da-he. Climate and environmental evolution of China [N]. Guangming Daily, 2007: [http://www.gmw.cn/01gmr/2007-07/05/content\\_634147.htm](http://www.gmw.cn/01gmr/2007-07/05/content_634147.htm).

- [22] ZHU Qian-gen, XIE Li-an. 1986-87 northern winter Asia/Australia circulation anomalies with their relation to the western Pacific SST [J]. *J. Trop. Meteor.*, 1988, 4: 254-262.
- [23] MULLEN S L. Transient eddy forcing of blocking flows [J]. *J. Atmos. Sci.*, 1987, 44: 3-22.
- [24] LU Ri-yu. Eddies during the blocking maintenance over the Northeastern Asian in summer [J]. *Chin. J. Atmos. Sci.*, 2001, 25(3): 289-302.
- [25] WATANABE M. Asian jet waveguide and a downstream extension of the North Atlantic Oscillation [J]. *J. Climate*, 2004, 17: 4 674-4 691.
- [26] HOSKINS B J, AMBRIZZI T. Rossby wave propagation on a realistic longitudinally varying flow [J]. *J. Atmos. Sci.*, 1993, 50:1 661-1 671.

**Citation:** WU Jun-jie, LIN Liang-xun, QIAN Yu-kun et al. A numerical diagnosis of leading signals facilitating a “north-ridge south-trough” dipole for the early-2008 South-China freezing-rain events. *J. Trop. Meteor.*, 2011, 17(2): 93-102.